Fabian Bamberg,[1,2,3] Holger Hetterich,[1,3] Susanne Rospleszcz,[4] Roberto Lorbeer,[1,3] Sigrid D. Auweter,[1] Christopher L. Schlett,[5] Anina Schafnitzel,[1] Christian Bayerl,[1] Andreas Schindler,[1] Tobias Saam,[1] Katharina Müller-Peltzer,[1] Wieland Sommer,[1] Tanja Zitzelsberger,[2] Jürgen Machann,[2,6,7] Michael Ingrisch,[1] Sonja Selder,[1] Wolfgang Rathmann,[8] Margit Heier,[4,9] Birgit Linkohr,[4] Christa Meisinger,[4,9] Christian Weber,[3,10] Birgit Ertl-Wagner,[1] Steffen Massberg,[11] Maximilian F. Reiser,[1] and Annette Peters[3,4,10]

Subclinical Disease Burden as Assessed by Whole-Body MRI in Subjects With Prediabetes, Subjects With Diabetes, and Normal Control Subjects From the General Population: The KORA-MRI Study

Diabetes 2017;66:158–169 | DOI: 10.2337/db16-0630

PATHOPHYSIOLOGY

Detailed pathophysiological manifestations of early disease in the context of prediabetes are poorly understood. This study aimed to evaluate the extent of early signs of metabolic and cardio-cerebrovascular complications affecting multiple organs in individuals with prediabetes. Subjects without a history of stroke, coronary artery disease, or peripheral artery disease were enrolled in a case-control study nested within the Cooperative Health Research in the Region of Augsburg (KORA) FF4 cohort and underwent comprehensive MRI assessment to characterize cerebral parameters (white matter lesions, microbleeds), cardiovascular parameters (carotid plaque, left ventricular function, and myocardial late gadolinium enhancement [LGE]), and metabolic parameters (hepatic proton-density fat fraction [PDFF] and subcutaneous and visceral abdominal fat). Among 400 subjects who underwent MRI, 103 subjects had prediabetes and 54 had established diabetes. Subjects with prediabetes had an increased risk for carotid plaque and adverse functional cardiac parameters, including reduced early diastolic filling rates as well as a higher prevalence of LGE compared with healthy control subjects. In addition, people with prediabetes had significantly elevated levels of PDFF and total and visceral fat. Thus, subjects with prediabetes show early signs of subclinical disease that include vascular, cardiac, and metabolic changes, as measured by whole-body MRI after adjusting for cardiometabolic risk factors.

The current epidemic of diabetes threatens the health of a large number of individuals in developed and developing countries (1). Most of the recent growth in the prevalence of diabetes can be attributed to an increase in type 2

[1]Institute of Clinical Radiology, Ludwig-Maximilian-University Hospital, Munich, Germany
[2]Department of Diagnostic and Interventional Radiology, University of Tübingen, Tübingen, Germany
[3]German Center for Cardiovascular Disease Research, Munich, Germany
[4]Institute of Epidemiology II, Helmholtz Zentrum München, German Research Center for Environmental Health, Neuherberg, Germany
[5]Department of Diagnostic and Interventional Radiology, University Hospital Heidelberg, Heidelberg, Germany
[6]Institute for Diabetes Research and Metabolic Diseases, Helmholtz Centre Tübingen, Tübingen, Germany
[7]German Centre for Diabetes Research, Tübingen, Germany
[8]Department of Biometry and Epidemiology, German Diabetes Center, Düsseldorf, Germany
[9]KORA Myocardial Infarction Registry, Central Hospital of Augsburg, Augsburg, Germany
[10]Institute for Cardiovascular Prevention, Ludwig-Maximilian-University Hospital, Munich, Germany
[11]Department of Cardiology, Ludwig-Maximilian-University Hospital, Munich, Germany
Corresponding author: Fabian Bamberg, fabian.bamberg@uni-tuebingen.de.

Received 17 May 2016 and accepted 4 October 2016.
This article contains Supplementary Data online at http://diabetes.diabetesjournals.org/lookup/suppl/doi:10.2337/db16-0630/-/DC1.
This article is featured in a podcast available at http://www.diabetesjournals.org/content/diabetes-core-update-podcasts.

diabetes, where insulin resistance and impaired insulin secretion are key features leading to well-known adverse cardiovascular outcomes (2). However, there is a large and increasing proportion of subjects (~20% of the adult U.S. population) who do not satisfy the diabetes criteria, but who still have impaired glucose metabolism and are thus classified as having prediabetes (3). These subjects are of particular relevance as they are at increased risk for either progressing to type 2 diabetes and/or cardiovascular events and may represent a beneficial prevention target (4). Their prevalence is expected to rise to almost 419 million worldwide by 2025 (5). However, detailed pathophysiological pathways of prediabetes as well as manifestations of early disease and its complications are not yet sufficiently understood.

Advanced imaging modalities, particularly whole-body MRI, provide the opportunity to visualize the parameters of subclinical disease and body composition without exposure to ionizing radiation. Because of technical advances, such as parallel acquisition techniques, continuous table movement techniques, and multichannel receiver coils, a comprehensive whole-body MRI protocol can be acquired within acceptable examination times and is increasingly established in clinical settings (6) as well as in population-based research (7).

In subjects with established diabetes, there is strong evidence that the level of detectable subclinical disease burden, such as myocardial perfusion and delayed enhancement as assessed by MRI, has strong prognostic relevance beyond left and right ventricular function (8–10). Less is known in subjects with prediabetes, although there is early evidence that prediabetes is associated with increased carotid plaque volume and arterial stiffness as determined by ultrasound (11,12), and changes in left ventricular (LV) function as determined by echocardiography (13,14) or native (15) or contrast-enhanced cardiac MRI (16). However, these observations lack, in part, a prospective design or reference group, comprise significant selection bias, or are not generalizable to a preventive setting. Nevertheless, they demonstrate that imaging can provide valuable insights into the disease process.

Thus, the aim of the current study was to determine the prevalence of early signs of subclinical cardiovascular disease in a cross-sectional study, using a dedicated cardiovascular whole-body MRI protocol, in subjects with prediabetes and diabetes, and in control subjects without known cardiovascular disease in a sample from the general population. Our hypothesis was that there is gradually increased subclinical disease burden among control subjects and subjects with prediabetes and diabetes.

RESEARCH DESIGN AND METHODS

Study Design

The study was designed as a cross-sectional case-control study nested in a prospective cohort from the Cooperative Health Research in the Region of Augsburg (KORA).

Subjects and Recruitment Procedure

Subjects who were 25–74 years of age were recruited between 1999 and 2001 from the FF4 follow-up of the KORA S4 study, a large sample from the general population in the region of Augsburg, Germany. The study design, sampling method, and data collection have been described in detail previously (17).

Eligible subjects were selected if they met the following inclusion criteria: willingness to undergo whole-body MRI; and qualification as being in the prediabetes, diabetes, or control group (see HEALTH ASSESSMENT). The following exclusion criteria were applied: age >72 years; subjects with validated/self-reported stroke, myocardial infarction, or revascularization; subjects with a cardiac pacemaker or implantable defibrillator, cerebral aneurysm clip, neural stimulator, any type of ear implant, an ocular foreign body, or any implanted device; pregnant or breast-feeding subjects; and subjects with claustrophobia, known allergy to gadolinium compounds, or serum creatinine level ≥1.3 mg/dL.

The study was approved by the institutional review board of the medical faculty of Ludwig-Maximilian University Munich, and all participants provided written informed consent.

Health Assessment

Subjects from the KORA S4 cohort were examined between June 2013 and September 2014 at the KORA study center. An oral glucose tolerance test (OGTT) was administered to all participants in whom type 2 diabetes had not been diagnosed. For the definition of prediabetes, the 1998 World Health Organization criteria were applied (18). Subjects with prediabetes had impaired glucose tolerance, as defined by a normal fasting glucose concentration and a 2-h serum glucose concentration, as determined by OGTT, ranging between 140 and 200 mg/dL; and/or an impaired fasting glucose concentration, as defined by fasting glucose levels between 110 and 125 mg/dL, and a normal 2-h serum glucose concentration. Individuals with a 2-h serum glucose concentration as determined by OGTT that was >200 mg/dL and/or a fasting glucose level that was >125 mg/dL were classified as having newly diagnosed diabetes. Subjects with normal glucose metabolism with a 2-h serum glucose concentration measured by OGTT that was <140 mg/dL and a fasting glucose level that was <110 mg/dL were classified as normal control subjects.

Other established risk factors were collected in standardized fashion as part of the KORA study design and have been described previously (17). Briefly, hypertension was defined as systolic blood pressure of at least 140 mmHg, diastolic blood pressure of at least 90 mmHg, or receiving current antihypertensive treatment. Subjects were classified as smokers if they reported current regular or sporadic cigarette smoking. BMI was defined as weight (kilograms) divided by the height squared (square meters). Medications were assigned as "antihypertensive medication" only if the compounds taken were classified as antihypertensively effective by the most recent guidelines. Antithrombotic medication comprised anticoagulant and antiplatelet drugs. Lipid-lowering medication was defined as statins, fibrates, or other lipid-modifying agents.

Assessment of Subclinical Disease by MRI

Subclinical disease manifestations were assessed by examinations on one MRI system at 3 Tesla (Magnetom Skyra; Siemens AG, Healthcare Sector, Erlangen, Germany) equipped with a whole-body radiofrequency coil-matrix system. All subjects underwent MRI within 3 months after their clinical examination at the study center. The whole-body protocol comprised sequences to cover the brain, cardiovascular system, and adipose tissue compartments of the chest and abdomen. Details on the MRI protocol are provided in Supplementary Table 1. All image analyses were performed in a blinded fashion by independent readers who were unaware of the diabetes status and clinical covariates using dedicated off-line workstations.

White Matter Lesions and Microbleeds

White matter lesions were graded on fluid-attenuated inversion recovery images according to the age-related white matter changes scale (ARWMC) in five brain areas in the left and right hemispheres, respectively (19). In each of the areas, the ordinal ARWMC score range was between 0 and 3. The presence of white matter lesions was defined as an ARWMC score >0 in any of the analyzed areas. The total ARWMC score was defined as the sum of scores of all areas, thereby ranging from 0 to 30. Total ARWMC score was square root transformed before analysis and treated as a continuous outcome. Microbleeds were defined as small foci of signal loss on a T2*-weighted sequence ($\geq$2 mm), and were counted in the lobar, deep, or infratentorial left or right hemisphere. Symmetric signal loss in the globus pallidum, most likely representing calcification, flow void artifact of the pial blood vessels, and intracerebral lesions with a hemorrhagic component were excluded.

Assessment of Carotid Plaque

Presence of plaque, measures of plaque burden, and gross composition of carotid plaque were determined on black-blood, T1-weighted, fat-suppressed sequences on both sides of the distal common carotid artery, at the carotid bulb, and in the proximal internal carotid artery, according to previously published criteria (20,21), which were established using histology as the gold standard. Boundaries of the vessel lumen and the vessel wall were analyzed for all 14 slice positions using commercially available semiautomatic software (CASCADE; University of Washington, Seattle, WA) (22). If necessary, manual corrections were performed. Qualitative criteria (American Heart Association [AHA]–Lesion Type, hemorrhage) were assessed for each side separately. The presence of calcification and hemorrhage, as well as wall thickness and wall eccentricity, were used to differentiate among type I, type III, type IV/V, and type VI/VII plaques.

LV Function

Cine-steady-state free precession sequences were evaluated semiautomatically using commercially available software (cvi42; Circle Cardiovascular Imaging, Calgary, Alberta, Canada) by two alternative readers. After automatic contour detection of the LV endocardium, all borders were corrected manually, if necessary, and according to current guidelines in order to avoid erroneous tracing of the myocardial border (23) (Supplementary Fig. 1). Reproducibility studies prior to this analysis revealed low inter-reader variability with relative differences of $<5\%$ for LV volumes and ejection fraction.

Filling and Ejection Rates

The time course of LV volume changes was quantified using associated gradients and time lags by using dedicated in-house software. This software displays the LV volume versus the time curve along with its derivative, and estimates peak gradients during early, passive LV filling and late LV filling due to atrial contraction, as detailed previously (24).

Late Gadolinium Enhancement

Analysis of the presence and characteristics of late gadolinium enhancement (LGE) was performed visually on fast low-angle shot inversion recovery sequences in short-axis stack and a four-chamber view by two experienced readers using commercially available software (cvi42; Circle Cardiovascular Imaging) for the presence and distribution pattern (subendocardial, midmyocardial, and epicardial) of LGE using the AHA 17-segment model (25). In case of discrepancy, a consensus reading was performed.

Hepatic Fat Content

Intrahepatic lipid content was quantified using multiecho single-voxel ($30 \times 30 \times 30$ mm^3) ^{1}H magnetic resonance spectroscopy, estimating proton-density fat fraction (PDFF) by accounting for the confounding effects of T2* decay and the spectral complexity of fat (26). Voxels were placed in the right (segment VIII) and left (segment II) liver lobes. Fat signal fraction was calculated by extrapolating fat and water integrals for an echo time of 0 ms using an exponential fit of values at five different values of echo time. PDFF was defined as the average of the right and left lobe measurements.

Body Adipose Tissue

On the basis of the volume-interpolated three-dimensional in/opposed-phase volumetric interpolated breath-hold examination–Dixon sequence, a fat-selective tomogram was calculated (slice thickness 5 mm in 5-mm increments). An in-house algorithm based on Matlab R2013a was used to semiautomatically quantify the total adipose tissue from the femoral head to the cardiac apex, visceral fat from the femoral head to the diaphragm, and subcutaneous adipose tissue from the femoral head to the cardiac apex (27). All segmentations were manually adjusted, if necessary. An example of adipose tissue segmentation is shown in Fig. 1.

Statistical Analysis

Subject demographics, cardiovascular risk factors, and MRI outcomes are presented as arithmetic means and SDs for continuous variables, and as counts and percentages for categorical variables. Hepatic fat outcomes were log transformed before analysis to meet the assumption of

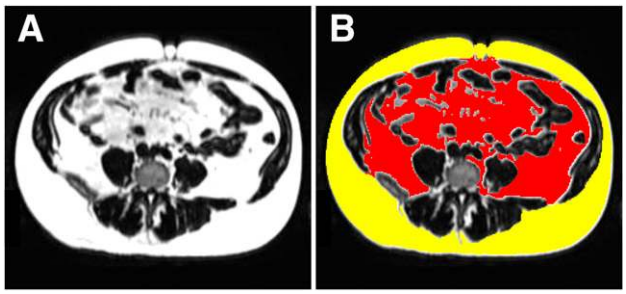

Figure 1—Adipose tissue segmentation. Example of the segmentation of adipose tissue at the level of the umbilicus of a 54-year-old male subject with a BMI of 28.7 kg/m^2. *A*: T1-weighted transaxial slice as the image source. *B*: Segmentation overlay with separation of visceral and subcutaneous adipose tissue (red and yellow, respectively). Visceral adipose tissue was 10.45 L.

normally distributed residuals and are therefore reported as geometric means and 95% CIs. Differences in baseline characteristics according to diabetes status were evaluated by one-way ANOVA and χ^2 test, respectively. Differences in mean MRI outcomes were assessed by a pairwise two-sample *t* test with pooled variance for continuous outcomes, and by χ^2 test or Fisher exact test for categorical outcomes. For all pairwise tests, Bonferroni correction was used to account for the two comparisons of the prediabetes and diabetes groups to the control group. To assess the association between diabetes status and each continuous MRI outcome, a linear regression model adjusted for age, sex, systolic blood pressure, smoking status, HDL cholesterol level, LDL cholesterol level, and triglyceride level was calculated. Diabetes status entered the model as a categorical variable with the three levels control, prediabetes, and diabetes, with the control group as the reference group. As additional sensitivity analyses, total ARWMC score was analyzed as count data by a zero-inflated negative binomial model, and median hepatic fat content was analyzed by quantile regression. For each outcome, adjusted least square mean values were calculated by inserting the mean population value of each covariate into the linear regression formula from the adjusted model.

Binary MRI outcomes were analyzed by logistic regression adjusted for the same variables as the linear models. For the binary outcome "presence of LGE" a logistic model based on penalized maximum likelihood with CIs based on profile likelihood was calculated (28). Categorical MRI outcomes were analyzed by ordered logistic regression with cumulative logit link under the proportional odds assumption (29). Estimates for all logistic models are reported as odds ratios (ORs). *P* values <0.05 were considered to indicate statistical significance. All analyses were conducted with R (version 3.2.1).

RESULTS

Among the 1,282 eligible subjects of the FF4 cohort, a total of 400 subjects underwent whole-body MRI, of whom 103 subjects were classified as people with prediabetes and 54 subjects had established diabetes (25.8% and 13.5%, respectively) (Fig. 2). On average, the mean examination time was 64.2 $\pm$ 10 min, and 12.3 $\pm$ 2.5 mL of contrast agent was administered, without differences among groups. Adverse events were observed in 1.25% (nausea in n = 5), and 2.5% aborted the examination prior to completion (n = 10). Examples of images displaying early signs of neurological, cardiovascular, and metabolic changes are provided in Figures 3, 4, and 5.

Demographic and risk profiles of the study participants (age 56.3 $\pm$ 9 years, 57.8% males) are provided in Table 1. Except for LDL levels, there were significant differences for the majority of parameters, including age, sex, and BMI, across the three groups.

Neurological Findings

Overall, the presence of white matter lesions was high (64%) and was significantly higher in subjects with diabetes compared with healthy control subjects and subjects with prediabetes (80% vs. 58% vs. 70%, respectively; P = 0.009) (Table 2). Also, subjects with prediabetes and diabetes had significantly higher ARWMC scores compared with healthy control subjects (1.56 $\pm$ 1.21 vs. 1.74 $\pm$ 1.12 vs. 1.14 $\pm$ 1.11, respectively; $P < 0.005$). However, these associations were attenuated after adjustment, and there was no difference in cerebral microbleeds among the groups (Table 3 and Supplementary Table 2). Results from the zero-inflated negative binomial model indicated the same associations as the main linear model.

Cardiovascular Findings

The presence of carotid plaque was higher in subjects with prediabetes (35%) compared with control subjects (17.5%, P = 0.024) and subjects with diabetes (16.7%). The type of plaque according to AHA classification was significantly different between control subjects and people with prediabetes (P = 0.033), where a diffuse intimal thickening or small eccentric plaque without calcification (AHA type III) was common (23.5% vs. 14% in people with prediabetes vs. control subjects) (Table 2). Prediabetes status was associated with carotid plaque burden after multivariable adjustment (OR 2.66, P = 0.016). An additional analysis that combined AHA type III/IV/V plaques into one category did not change this finding.

In univariate analysis, significant differences of functional LV parameters were detected among the groups with respect to both mean and variance (Fig. 6 and Table 2). After adjustment, significantly lower end-diastolic volumes, end-systolic volumes, stroke volumes, and peak ejection rates were observed both for subjects with prediabetes and for subjects with diabetes (all $P < 0.001$ when compared with healthy control subjects) (Table 3 and Supplementary Table 2). Early and late diastolic filling rates decreased from subjects with prediabetes to those with diabetes compared with healthy control subjects, although only early filling rates were significantly reduced in subjects with prediabetes.

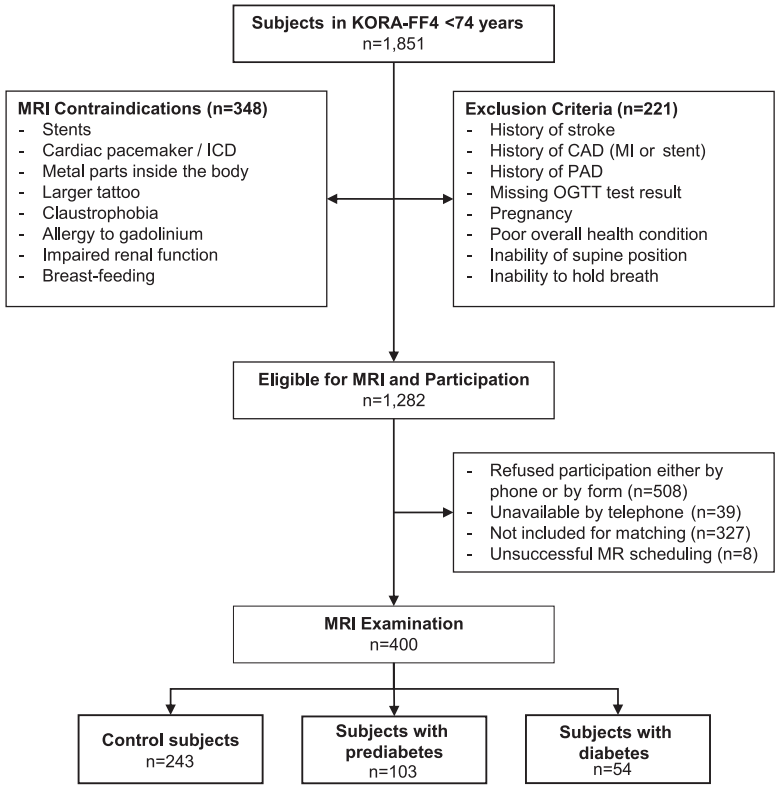

Figure 2—Participant flow diagram. Among the 1,282 eligible subjects in the FF4 cohort, a total of 400 subjects underwent whole-body MRI. ICD, implantable cardioverter defibrillator; MI, myocardial infarction; PAD, peripheral artery disease.

Myocardial mass was significantly increased in subjects with prediabetes and diabetes compared with control subjects in univariate analysis (all P values <0.001). These differences were attenuated after adjustment and became nonsignificant. LGE was present in 2.9% of subjects, with a total of 34 affected segments. Of those, the majority

Table 1—Subject demographics and cardiovascular risk factors

	All (N = 400)	Control subjects (N = 243)	Subjects with prediabetes (N = 103)	Subjects with diabetes (N = 54)	P value
Age (years)	56.3 ± 9	54.2 ± 9	58.3 ± 9	61.8 ± 8	**<0.001**
Male sex	231 (57.8%)	125 (51.4%)	66 (64.1%)	40 (74.1%)	**0.003**
BMI (kg/m^2)	28.1 ± 5	26.7 ± 4	30.5 ± 5	30.2 ± 5	**<0.001**
Smoking					0.2
Never smoker	146 (36.5%)	95 (39.1%)	34 (33.0%)	17 (31.5%)	
Ex-smoker	174 (43.5%)	94 (38.7%)	51 (49.5%)	29 (53.7%)	
Smoker	80 (20.0%)	54 (22.2%)	18 (17.5%)	8 (14.8%)	
Systolic BP (mmHg)	120.6 ± 16	116.7 ± 15	124.3 ± 15	131.2 ± 21	**<0.001**
Diastolic BP (mmHg)	75.3 ± 10	73.8 ± 9	77.5 ± 10	77.6 ± 13	**<0.001**
Hypertension	136 (34.0%)	51 (21.0%)	47 (45.6%)	38 (70.4%)	**<0.001**
Total cholesterol (mg/dL)	217.8 ± 36	216.1 ± 36	223.8 ± 32	214.4 ± 45	0.2
HDL (mg/dL)	61.9 ± 18	65.2 ± 18	58.5 ± 14	53.7 ± 19	**<0.001**
LDL (mg/dL)	139.5 ± 33	138.4 ± 32	144.6 ± 30	134.7 ± 41	0.2
Triglycerides (mg/dL)	131.5 ± 85	107.4 ± 64	151.8 ± 81	201.2 ± 121	**<0.001**
Antihypertensive med	102 (25.5%)	41 (16.9%)	34 (33.0%)	27 (50.0%)	**<0.001**
Antithrombotic med	23 (5.8%)	7 (2.9%)	7 (6.8%)	9 (16.7%)	**<0.001**
Lipid-lowering med	43 (10.8%)	16 (6.6%)	9 (8.7%)	18 (33.3%)	**<0.001**

Values are reported as the mean ± SD or n (%), unless otherwise indicated. Significant values are shown in bold. BP, blood pressure; med, medication.

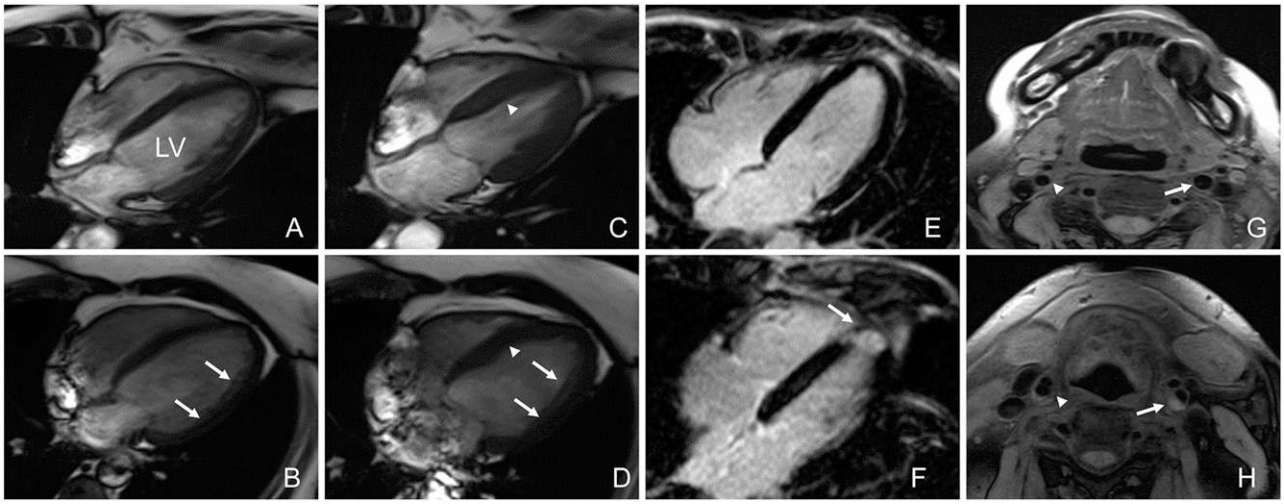

Figure 3—Examples of cardiovascular findings. Findings of subclinical disease burden as detected by MRI in control subjects (top row) and subjects with variable findings (bottom row). Typical diastolic (*A*) and systolic (*C*) myocardial thickening and contraction compared with dilated diastolic configuration of the LV with impaired contraction and thickening of the lateral wall (arrows) and the septum (arrowheads) (*B* and *D*). On LGE, there was no evidence of ischemic enhancement (*E*) compared with a transmural apical enhancement (arrow, *F*). Normal visualization of the right (arrowhead) and left common carotid artery (arrow, *G*) compared with evidence of atherosclerotic plaque in the left common carotid artery (arrow, *H*).

(65%) were classified as subendocardial and midmyocardial, and 18% were classified as transmural. The prevalence of LGE was significantly higher in subjects with prediabetes and diabetes compared with healthy control subjects (Table 2). The difference remained significant in subjects with diabetes after adjusting for age and sex (OR 4.46, $P = 0.04$).

Metabolic Findings

Strong associations were detected with respect to the amount of hepatic lipids and adipose tissue between the groups (Fig. 7). The PDFF was highest in subjects with diabetes and lowest in healthy subjects (12.9% vs. 4.1%, $P < 0.001$), but also was significantly increased in subjects with prediabetes (9.6%, $P < 0.001$). Not only the mean PDFF, but also its variance increased when comparing individuals with prediabetes and diabetes to healthy control subjects. These differences persisted after adjustment. The results of quantile regression were consistent with the results of linear regression. Similarly, total adipose tissue and visceral adipose tissue were independently higher in subjects with prediabetes and diabetes (all P values <0.001), while after adjustment for BMI the differences for subcutaneous adipose tissue were attenuated (coefficient: prediabetes 0.32, diabetes 0.38).

DISCUSSION

In this nested case-control study, we describe the subclinical disease burden, as measured by whole-body MRI,

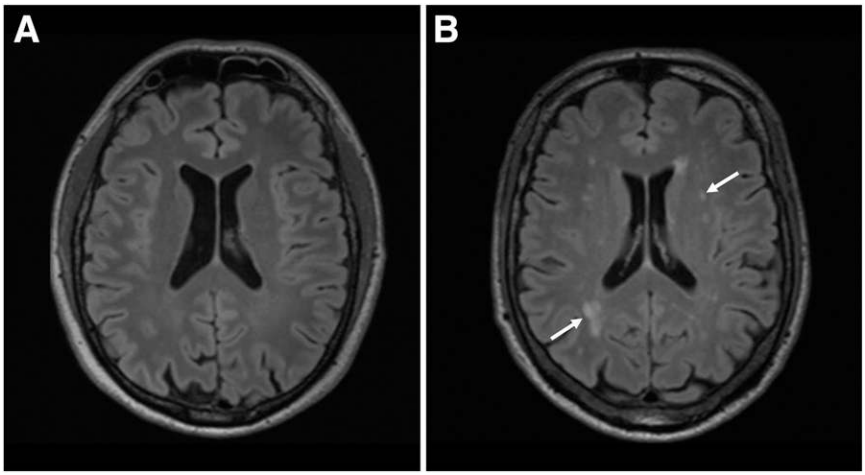

Figure 4—Example of cerebral findings. Fluid-attenuated inversion recovery sequences demonstrating absence and presence of white matter lesions in a healthy subject (*A*) compared with a subject with prediabetes (*B*, arrows), respectively.

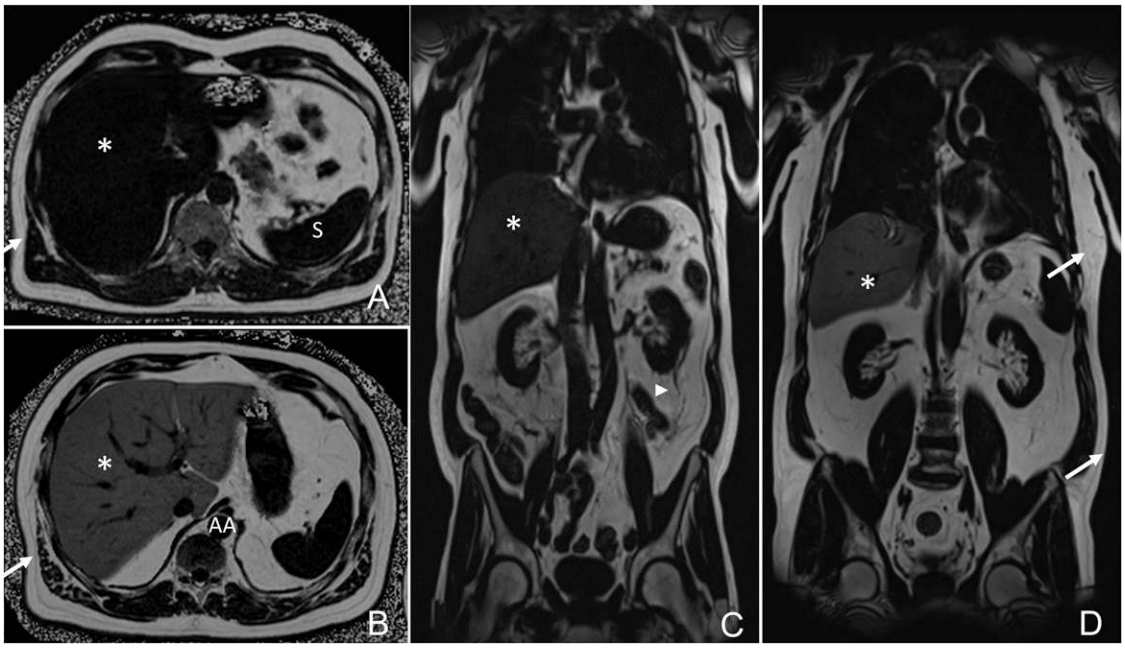

Figure 5—Examples of metabolic findings. Differences in hepatic fat content based on a multiecho DIXON sequence demonstrating normal signal (*A*) and attenuated signal due to steatosis (33% PDFF, *B*), and subcutaneous (arrows) and visceral (arrowhead) adipose tissue between a healthy control subject and a subject with prediabetes (*A–D*). *Liver. AA, abdominal aorta; S, spleen.

for subjects with prediabetes and diabetes compared with healthy control subjects who were selected based on a population-based cohort study. Our results indicate that there are substantial differences, not only in subjects with established diabetes but also in subjects with prediabetes. Thus, our results provide further insight into the extent of early signs of complications in subjects with prediabetes and indicate that, besides strong metabolic differences, there are manifest subclinical disease states, particularly in the cardiovascular system.

While it is established that diabetes represents a major current and future risk to cardiovascular health, the risk for subjects with impaired glucose metabolism who are not classified as having diabetes remains less clear. The prevalence of prediabetes is on the rise; it is estimated that prediabetes will have a prevalence of almost 419 million worldwide by 2025 (5) and, therefore, is predicted to be of major concern in aging populations. Thus, an improved understanding and prevention strategies are required to target the underlying disease mechanisms and to prevent complications.

The observation that subjects with prediabetes have detectable changes to the cardiovascular system is not novel, as microvascular and macrovascular disease states have been described in different studies, using ultrasound for the assessment of carotid plaque volume and arterial stiffness (11,12), echocardiography for the assessment of LV function (13,14), or native (15) or contrast-enhanced cardiac MRI (16). Our results confirm and extend the findings of these earlier reports in a relatively large sample drawn from a Western European general population by demonstrating a continuous increase in subclinical disease burden ranging from healthy control subjects to people with prediabetes to people with diabetes for the majority of the obtained parameters. In contrast to earlier reports with limited organ coverage, we applied a comprehensive, nonionizing imaging modality to cover the various organ systems. Our results indicate that a systemic, whole-body approach might help in predicting an individual's risk in the setting of diabetes; however, this needs to be tested in prospective studies. While it is known, for instance, that polyvascular involvement is associated with significantly higher rates of major adverse events than in single-site vascular disease (30), our findings add a new level of information pertaining to different organ systems and including metabolic phenotypes. This may represent the multifactorial, individual course of natural disease development (31,32), and is a unique opportunity to characterize a metabolic disease affecting the whole body more accurately. In fact, currently launched, large prospective cohort studies provide the basis to estimate risk associated with these MRI findings (33,34).

To date, it remains unclear whether elevated glucose levels in the setting of prediabetes are a direct cause of clinical cardiovascular disease or contribute to the cardiovascular risk by their relationship to cardiovascular risk factors (35). In a meta-analysis, Ford et al. (36) found that available data are characterized by substantial heterogeneity resulting in a moderate summary relative risk of 1.20 (95% CI 1.12, 1.28) associated with the presence of prediabetes. Most of this can be attributed to the presence of many confounding variables, such as concomitant obesity, dyslipidemia, or hypertension, which limit the assessment

Table 2—Difference in subclinical disease burden between subjects with prediabetes, subjects with diabetes, and healthy control subjects

	All	Control subjects	Subjects with prediabetes	*P* value*	Subjects with diabetes	*P* value**
Brain						
White matter lesions	247 (64.0%)	138 (58.0%)	68 (70.1%)	0.1	41 (80.4%)	**0.009**
Cerebral microbleeds	49 (12.8%)	27 (11.4%)	12 (12.5%)	1	10 (20.0%)	0.3
Total ARWMC score	1.33 ± 1.16	1.14 ± 1.11	1.56 ± 1.21	**0.005**	1.74 ± 1.12	**0.001**
Carotid plaque						
Presence of plaque	55 (20.8%)	30 (17.5%)	18 (35.3%)	**0.02**	7 (16.7%)	1
Presence of plaque type						
AHA type I	209 (79.2%)	141 (82.5%)	33 (64.7%)	**0.03**	35 (83.3%)	0.09
AHA type III	39 (14.8%)	24 (14.0%)	12 (23.5%)		3 (7.1%)	
AHA type V	10 (3.8%)	2 (1.2%)	4 (7.8%)		4 (9.5%)	
AHA type VI or VII	6 (2.3%)	4 (2.3%)	2 (3.9%)		0 (0.00%)	
Wall thickness, LCA (mm)	0.75 ± 0.11	0.73 ± 0.09	0.77 ± 0.11	0.06	0.79 ± 0.14	**0.006**
Wall thickness, RCA (mm)	0.76 ± 0.10	0.75 ± 0.10	0.77 ± 0.09	0.2	0.78 ± 0.11	0.09
Cardiac function						
Early diastolic filling rate (mL/s)	225.7 ± 115.2	255.8 ± 122.8	190.0 ± 86.1	**<0.001**	156.9 ± 72.8	**<0.001**
Late diastolic filling rate (mL/s)	226.8 ± 109.2	237.3 ± 114.6	223.9 ± 103.9	0.6	180.5 ± 77.3	**0.002**
End-diastolic volume (mL/m^2)	66.3 ± 15.0	70.2 ± 14.5	60.8 ± 12.7	**<0.001**	58.6 ± 15.4	**<0.001**
End-systolic volume (mL/m^2)	20.8 ± 8.7	22.4 ± 8.2	17.9 ± 7.4	**<0.001**	19.1 ± 11.1	**0.03**
Stroke volume (mL/m^2)	45.4 ± 9.7	47.8 ± 9.9	42.9 ± 7.9	**<0.001**	39.6 ± 8.8	**<0.001**
Ejection fraction (%)	69.2 ± 8.1	68.5 ± 7.9	71.3 ± 7.7	**0.008**	68.5 ± 9.6	1
Peak ejection rate (mL/s)	354.1 ± 132.9	378.5 ± 139.1	337.5 ± 113.6	**0.02**	272.4 ± 99.4	**<0.001**
Myocardium						
Myocardial mass (g/m^2)	72.9 ± 15.5	70.4 ± 15.7	75.9 ± 13.8	**0.006**	78.6 ± 15.8	**0.001**
LGE	11 (2.9%)	2 (0.9%)	6 (6.0%)	**0.03**	3 (6.3%)	**0.01**
Hepatic fat content						
PDFF (%)	6.0 (5.4, 6.5)	4.1 (3.7, 4.5)	9.6 (8.2, 11.3)	**<0.001**	12.9 (10.3, 16.1)	**<0.001**
Body adipose tissue (L)						
Total adipose tissue	12.6 ± 5.4	10.7 ± 4.7	15.3 ± 5.3	**<0.001**	16.0 ± 5.4	**<0.001**
Subcutaneous adipose tissue	8.1 ± 3.8	7.3 ± 3.2	9.6 ± 4.2	**<0.001**	9.2 ± 3.8	**0.001**
Visceral adipose tissue	4.5 ± 2.7	3.5 ± 2.3	5.8 ± 2.4	**<0.001**	6.9 ± 2.4	**<0.001**

Values are reported as the mean ± SD, *n* (%), or OR (95% CI), unless otherwise indicated. Significant values are shown in bold. LCA, left carotid artery; RCA, right carotid artery. *Against control subjects. **Against control subjects.

of a direct association. Our results also indicate that the presence of confounding factors increases from healthy control subjects to people with prediabetes to people with diabetes (Table 1). In order to compensate for these confounders, we performed multivariable adjustment and found that changes to the cardiovascular system (carotid plaque burden, cardiac functional parameters) as well as metabolic changes (hepatic steatosis and visceral adipose tissue) remained highly elevated in subjects with prediabetes. Thus, our results add to the hypothesis that elevated glucose levels in prediabetes have a direct relationship to microvascular and macrovascular disease, and may require more medical attention and preventive treatment. It is important to note that by selecting subjects with diabetes without any overt cardiovascular disease, we are investigating a very specific subgroup. This is reflected in the risk for detecting carotid plaques, which was increased in subjects with prediabetes, but was nonsignificantly altered in subjects with diabetes. With atherosclerosis being a systemic disease, the number of subjects with advanced atherosclerotic plaques in the carotid arteries might have been artificially lowered. These circumstances may explain the overall low number of plaques in the study and especially in the high-risk diabetes group, since diabetes is a known risk factor for accelerated plaque development. Specifically, we found increased rates of myocardial LGE in subjects with prediabetes, predominantly representing minor myocardial infarctions by their location (65% subendocardial, 18% transmural). In a retrospective analysis in 181 patients, Yoon et al. (16) found a prevalence of LGE in patients with prediabetes of 25% (compared with 35% in patients with diabetes). Compared with our findings, the prevalence reported by Yoon et al. (16) is significantly higher, and because of our low numbers we were unable to present fully adjusted results. One explanation for the observed difference between the studies is that these subjects were referred for suspected cardiac disease and that many of them had established coronary artery disease (CAD) (~36%), also evident by the rate of subsequent revascularizations (25.4%). In contrast, our sample was recruited from the general population without established CAD, which may be more generalizable in a preventive setting. Thus, further research is required to confirm that postischemic myocardial changes are a predominant feature of the prediabetic state.

Table 3—Results of regression model adjusted for age, sex, systolic blood pressure, BMI, smoking status, and levels of HDL, LDL, and triglycerides

	Subjects with prediabetes			Subjects with diabetes		
	Estimate	95% CI	*P* value	Estimate	95% CI	*P* value
Brain						
White matter lesions	OR 1.18	(0.65, 2.16)	0.6	OR 1.58	(0.67, 3.96)	0.3
Cerebral microbleeds	OR 1.20	(0.52, 2.69)	0.7	OR 1.99	(0.72, 5.33)	0.2
Total ARWMC score	0.21	(−0.07, 0.48)	0.1	0.20	(−0.17, 0.58)	0.3
Carotid plaque						
Presence of plaque (%)	OR 2.66	(1.20, 5.90)	**0.02**	OR 0.68	(0.22, 1.94)	0.5
Plaque type	OR 2.57	(1.17, 5.61)	**0.02**	OR 0.65	(0.21, 1.88)	0.5
Wall thickness, LCA (mm)	0.0086	(−0.03, 0.04)	0.6	0.019	(−0.02, 0.06)	0.4
Wall thickness, RCA (mm)	−0.0023	(−0.04, 0.03)	0.9	−0.009	(−0.05, 0.03)	0.6
Cardiac function						
Early filling rate (mL/s)	−38.97	(−65.87, −12.06)	**0.005**	−56.46	(−93.34, −19.59)	**0.003**
Late filling rate (mL/s)	−27.17	(−54.56, 0.22)	0.05	−68.31	(−106.89, −29.73)	**<0.001**
End-diastolic volume (mL/m^2)	−7.20	(−10.8, −3.59)	**<0.001**	−9.45	(−14.39, −4.51)	**<0.001**
End-systolic volume (mL/m^2)	−4.26	(−6.43, −2.1)	**<0.001**	−3.17	(−6.14, −0.19)	**0.04**
Stroke volume (mL/m^2)	−3.01	(−5.35, −0.67)	**0.01**	−6.18	(−9.38, −2.98)	**<0.001**
Ejection fraction (%)	3.36	(1.28, 5.44)	**0.001**	0.82	(−2.03, 3.66)	0.6
Peak ejection rate (mL/s)	−33.67	(−66.31, −1.03)	**0.04**	−93.6	(−138.33, −48.88)	**<0.001**
Myocardium						
Myocardial mass (g/m^2)	0.96	(−2.26, 4.17)	0.6	−0.05	(−4.46, 4.36)	1
Hepatic fat content						
PDFF (%)	GMR 1.49	(1.26, 1.77)	**<0.001**	GMR 1.7	(1.35, 2.14)	**<0.001**
Body adipose tissue (L)						
Total adipose tissue	0.87	(0.26, 1.49)	**0.006**	1.34	(0.5, 2.18)	**0.002**
Subcutaneous adipose tissue	0.32	(−0.1, 0.74)	0.1	0.38	(−0.2, 0.95)	0.2
Visceral adipose tissue	0.50	(0.11, 0.89)	**0.001**	0.92	(0.4, 1.44)	**0.001**

Estimates represent β-estimates from linear regression if not otherwise specified. GMR, geometric mean ratio. Significant values are shown in bold.

We confirm earlier results from the Multi-Ethnic Study of Atherosclerosis (MESA) by Shah et al. (15), showing that prediabetes (impaired fasting glucose) is associated with concentric LV remodeling independent of BMI (β = 0.02 kg/m^2, $P = 0.04$) in a much larger sample. Our findings also demonstrate that there are significantly abnormal functional LV parameters in people with prediabetes compared with healthy control subjects, indicating early systolic and diastolic myocardial remodeling (i.e., end-diastolic volume, end-systolic volume, stroke volume, and peak ejection rate). In addition, we show that these parameters of myocardial remodeling, in particular stroke volume and peak ejection rate, are even more pronounced in diabetes, which may indicate a disease continuum. Early LV filling rate is lowered in subjects with prediabetes and diabetes, suggesting an increasing severity with the progression of disease. A

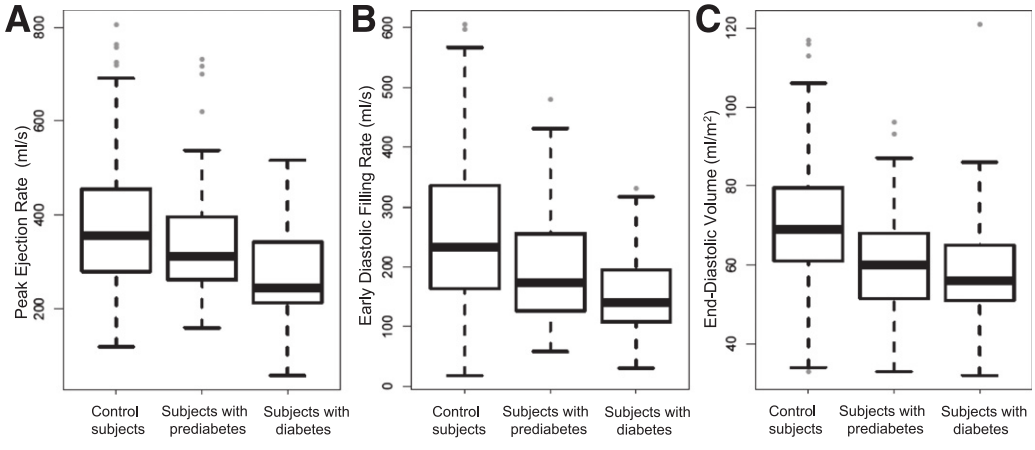

Figure 6—Cardiac function. Observed peak ejection rates (*A*), early diastolic filling rates (*B*), and end-diastolic volumes (*C*) among subjects with prediabetes, subjects with diabetes, and healthy control subjects (all $P < 0.001$).

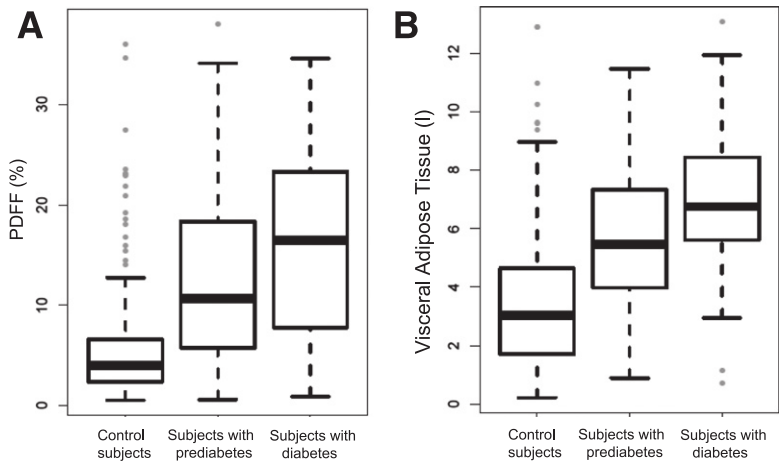

Figure 7—Metabolic imaging results. Observed hepatic fat content measured as PDFF (*A*) and visceral adipose tissue (*B*) among subjects with prediabetes, subjects with diabetes, and healthy control subjects (all $P < 0.001$).

similar trend was observed for late LV filling rates, but the results in individuals with prediabetes were only borderline significant. These findings potentially indicate early signs of the development of diabetic cardiomyopathy (37,38).

While in the MESA trial (15) similar associations were observed for waist-to-hip ratio, we demonstrate that the visceral adipose tissue particularly is significantly increased in subjects with prediabetes with again increased volume in subjects with diabetes (by 0.5 L and by 1.09 L compared with healthy control subjects, respectively) independent of BMI. With this, we also confirm earlier findings in the Framingham Heart Study (39) using computed tomography, indicating that visceral adipose tissue is more strongly associated with an adverse metabolic risk profile even after accounting for standard anthropometric indexes. Moreover, our results show that subjects with prediabetes have significantly increased hepatic fat content compared with healthy control subjects (with again increased values in subjects with diabetes). In fact, on average the predicted PDFF was 7.1% (95% CI 6.2, 8.2%) in subjects with prediabetes, indicating that the vast majority of these subjects are categorized as having fatty liver disease with its associated risk of morbidity (40).

We did not find any independent differences of white matter lesions and cerebral microbleeds between subjects with prediabetes and control subjects, despite some associations in crude analysis. Although white matter lesions and cerebral microbleeds are known to be associated with diabetes (41), further research will be necessary to confirm that these postischemic changes do not play a predominant role in prediabetes.

Notably, although we observed clear evidence for subclinical changes in the heart and the fat distribution, our results indicate that there is substantial variability of subclinical disease among subjects with prediabetes for other nonmetabolic phenotypes, which has also been observed in other studies (42). However, for cardiac outcomes, normal control subjects displayed higher variability than the individuals with prediabetes or diabetes. Thus, one possible explanation for the very heterogeneous relative risk observed in longitudinal studies (35) may be that the effect of prediabetes differs depending on the varying degree of subclinical disease manifestation. The data presented here suggest that comprehensive imaging is able to characterize the increased systemic subclinical disease burden in subjects with prediabetes and subjects with diabetes compared with control subjects. Moreover, we also show that, even among subjects with prediabetes, the MR phenotype is heterogeneous. It can be speculated that these heterogeneous MR phenotypes have the potential to risk stratify and tailor preventive measures within the context of personalized medicine, if their predictive power is confirmed in longitudinal analysis (43).

By demonstrating that there are quantitative measures that can be obtained from such a standardized whole-body MRI protocol, we also provide a basis for the emerging field of radiomics (44). Initially driven by oncological disease characterization, more comprehensive disease and risk characterization by advanced imaging postprocessing will further increase the predictive power of the obtained imaging data. One example may represent the MR phenotype of visceral fat, a well-established correlate of cardiometabolic risk. Besides reporting on volume, it can be anticipated that additional radiomics-based parameters, including shape, intensity, and texture features, will provide incremental value in more accurately risk stratifying cardiometabolic patients.

The results of this study need to be interpreted in light of its limitations. The current analysis is of a cross-sectional nature and aimed to identify MRI parameters as early pathophysiological markers of disease. We do not provide risk estimates of the prognostic relevance of the MRI findings. Our study has a limited sample size, and further studies with larger sets of individuals with prediabetes and diabetes are required to confirm our results. We applied contrast-enhanced whole-body MRI as a means to assess subclinical disease burden. Although this is advantageous with respect to its high temporal, spatial, and

soft-tissue resolution, the technique is associated with contraindications, which precluded a number of subjects from participation (Fig. 2). Our applied slice thickness of 8 mm does not allow for continuous phenotyping of the left ventricle; however, it will be subject to future research to determine the value of a true three-dimensional volumetric assessment. Because of the limited scanning time allotted by the institutional review board, a number of other MR sequences with potential scientific value in the setting of prediabetes and diabetes had to be excluded.

Although all traditional cardiovascular risk factors, such as obesity, dyslipidemia, or hypertension, were included in the analysis model, the existence of unmeasured confounding variables cannot be fully ruled out. However, our comprehensive approach to consider risk factors suggests that prediabetes and diabetes add independently of obesity and hypertension to the development of complications. Nevertheless, the effect of prediabetes and diabetes on MRI outcomes might be driven by a specific aspect of the respective glycemic status, such as the HbA_{1c} value, insulin levels, or glucose levels. However, we felt that it was more appropriate to use the categories control, prediabetes, and diabetes as clinical entities, as given by the chosen study design. Furthermore, our sample size is not sufficient to support a model with too many and possibly highly correlated variables.

In conclusion, subjects with prediabetes free from overt cardiovascular disease derived from a population-based cohort study have an independent increased risk for vascular, cardiac, and metabolic changes, as measured by MRI, providing evidence for increased subclinical disease burden. These changes are frequently more advanced in subjects with established diabetes, highlighting the notion that—similar to diabetes—prediabetes is a systemic state affecting many organ systems. From a clinical perspective, whole-body MRI thus represents an imaging modality to detect early functional and structural changes that are indicative of complication development beyond the traditional assessment of risk factors, such as obesity, dyslipidemia, or hypertension. Overall, these findings suggest that individuals with prediabetes need more comprehensive assessments for signs of early pathophysiological changes, tailored preventive measures, and adequate treatment not only to abate the underlying development of diabetes, but also to avoid the development of cardiac complications.

Funding. This study was funded by German Research Foundation (Bonn, Germany) grant BA 4233/4-1, and German Centre for Cardiovascular Disease Research (Berlin, Germany) grants 81X2600209 and 81X2600214.

Duality of Interest. No potential conflicts of interest relevant to this article were reported.

Author Contributions. F.B. and H.H. conceived and designed the study; collected, analyzed, and interpreted the data; and drafted the article. S.R. and R.L. analyzed and interpreted the data and drafted the article. S.D.A. collected the data and drafted the article. C.L.S. contributed to critical revision of the article. A.Scha., C.B., A.Schi., T.S., K.M.-P., W.S., T.Z., J.M., M.I., S.S., W.R., M.H., B.L., and C.M. contributed to data collection and critical revision of the article. C.W., B.E.-W., S.M., and M.F.R. conceived and designed the study and contributed to critical revision of the article. A.P. conceived and designed the study, analyzed and interpreted the data, and contributed to critical revision of the article. All authors gave final approval of the version of the article to be published. F.B. and A.P. are the guarantors of this work and, as such, had full access to all the data in the study and take responsibility for the integrity of the data and the accuracy of the data analysis.

References

1. King H, Aubert RE, Herman WH. Global burden of diabetes, 1995-2025: prevalence, numerical estimates, and projections. Diabetes Care 1998;21:1414–1431
2. Nathan DM, Davidson MB, DeFronzo RA, et al.; American Diabetes Association. Impaired fasting glucose and impaired glucose tolerance: implications for care. Diabetes Care 2007;30:753–759
3. Cowie CC, Rust KF, Byrd-Holt DD, et al. Prevalence of diabetes and impaired fasting glucose in adults in the U.S. population: National Health And Nutrition Examination Survey 1999-2002. Diabetes Care 2006;29:1263–1268
4. Danaei G, Lawes CM, Vander Hoorn S, Murray CJ, Ezzati M. Global and regional mortality from ischaemic heart disease and stroke attributable to higher-than-optimum blood glucose concentration: comparative risk assessment. Lancet 2006;368:1651–1659
5. Alberti KG. Screening and diagnosis of prediabetes: where are we headed? Diabetes Obes Metab 2007;9(Suppl. 1):12–16
6. Pasoglou V, Michoux N, Peeters F, et al. Whole-body 3D T1-weighted MR imaging in patients with prostate cancer: feasibility and evaluation in screening for metastatic disease. Radiology 2015;275:155–166
7. Bamberg F, Kauczor HU, Weckbach S, et al.; German National Cohort MRI Study Investigators. Whole-body MR imaging in the German national cohort: rationale, design, and technical background. Radiology 2015;277:206–220
8. Hundley WG. The use of cardiovascular magnetic resonance to identify adverse cardiac prognosis: an important step in reducing image-related health care expenditures. J Am Coll Cardiol 2010;56:1244–1246
9. Kwong RY, Sattar H, Wu H, et al. Incidence and prognostic implication of unrecognized myocardial scar characterized by cardiac magnetic resonance in diabetic patients without clinical evidence of myocardial infarction. Circulation 2008;118:1011–1020
10. Bamberg F, Parhofer KG, Lochner E, et al. Diabetes mellitus: long-term prognostic value of whole-body MR imaging for the occurrence of cardiac and cerebrovascular events. Radiology 2013;269:730–737
11. Faeh D, William J, Yerly P, Paccaud F, Bovet P. Diabetes and pre-diabetes are associated with cardiovascular risk factors and carotid/femoral intima-media thickness independently of markers of insulin resistance and adiposity. Cardiovasc Diabetol 2007;6:32
12. Schram MT, Henry RM, van Dijk RA, et al. Increased central artery stiffness in impaired glucose metabolism and type 2 diabetes: the Hoorn Study. Hypertension 2004;43:176–181
13. Fox ER, Sarpong DF, Cook JC, et al. The relation of diabetes, impaired fasting blood glucose, and insulin resistance to left ventricular structure and function in African Americans: the Jackson Heart Study. Diabetes Care 2011;34:507–509
14. Stahrenberg R, Edelmann F, Mende M, et al. Association of glucose metabolism with diastolic function along the diabetic continuum. Diabetologia 2010; 53:1331–1340
15. Shah RV, Abbasi SA, Heydari B, et al. Insulin resistance, subclinical left ventricular remodeling, and the obesity paradox: MESA (Multi-Ethnic Study of Atherosclerosis). J Am Coll Cardiol 2013;61:1698–1706
16. Yoon YE, Kitagawa K, Kato S, et al. Prognostic significance of unrecognized myocardial infarction detected with MR imaging in patients with impaired fasting glucose compared with those with diabetes. Radiology 2012;262:807–815
17. Holle R, Happich M, Löwel H, Wichmann HE; MONICA/KORA Study Group. KORA—a research platform for population based health research. Gesundheitswesen 2005;67(Suppl. 1):S19–S25
18. World Health Organization, International Diabetes Federation. *Definition and Diagnosis of Diabetes Mellitus and Intermediate Hyperglycemia: Report of a WHO/IDF Consultation*. Geneva, Switzerland, World Health Organization, 2006, p. 13–28

19. Wahlund LO, Barkhof F, Fazekas F, et al.; European Task Force on Age-Related White Matter Changes. A new rating scale for age-related white matter changes applicable to MRI and CT. Stroke 2001;32:1318–1322
20. Cai JM, Hatsukami TS, Ferguson MS, Small R, Polissar NL, Yuan C. Classification of human carotid atherosclerotic lesions with in vivo multicontrast magnetic resonance imaging. Circulation 2002;106:1368–1373
21. Saam T, Ferguson MS, Yarnykh VL, et al. Quantitative evaluation of carotid plaque composition by in vivo MRI. Arterioscler Thromb Vasc Biol 2005;25:234–239
22. Kerwin W, Xu D, Liu F, et al. Magnetic resonance imaging of carotid atherosclerosis: plaque analysis. Top Magn Reson Imaging 2007;18:371–378
23. Schulz-Menger J, Bluemke DA, Bremerich J, et al. Standardized image interpretation and post processing in cardiovascular magnetic resonance: Society for Cardiovascular Magnetic Resonance (SCMR) board of trustees task force on standardized post processing. J Cardiovasc Magn Reson 2013;15:35
24. Caudron J, Fares J, Bauer F, Dacher JN. Evaluation of left ventricular diastolic function with cardiac MR imaging. Radiographics 2011;31:239–259
25. Hundley WG, Bluemke DA, Finn JP, et al.; American College of Cardiology Foundation Task Force on Expert Consensus Documents. ACCF/ACR/AHA/NASCI/SCMR 2010 expert consensus document on cardiovascular magnetic resonance: a report of the American College of Cardiology Foundation Task Force on Expert Consensus Documents. J Am Coll Cardiol 2010;55:2614–2662
26. Hetterich H, Bayerl C, Peters A, et al. Feasibility of a three-step magnetic resonance imaging approach for the assessment of hepatic steatosis in an asymptomatic study population. Eur Radiol 2016;26:1895–1904
27. Würslin C, Machann J, Rempp H, Claussen C, Yang B, Schick F. Topography mapping of whole body adipose tissue using A fully automated and standardized procedure. J Magn Reson Imaging 2010;31:430–439
28. Firth D. Bias reduction of maximum likelihood estimates. Biometrika 1993;80:27–38
29. Agresti A, Kateri M. *Categorical Data Analysis*. New York, Springer, 2011
30. Bhatt DL, Eagle KA, Ohman EM, et al.; REACH Registry Investigators. Comparative determinants of 4-year cardiovascular event rates in stable outpatients at risk of or with atherothrombosis. JAMA 2010;304:1350–1357
31. van der Meer RW, Lamb HJ, Smit JW, de Roos A. MR imaging evaluation of cardiovascular risk in metabolic syndrome. Radiology 2012;264:21–37
32. Gatidis S, Schlett CL, Notohamiprodjo M, Bamberg F. Imaging-based characterization of cardiometabolic phenotypes focusing on whole-body MRI—an approach to disease prevention and personalized treatment. Br J Radiol 2016;89:20150829
33. Petersen SE, Matthews PM, Francis JM, et al. UK Biobank's cardiovascular magnetic resonance protocol. J Cardiovasc Magn Reson 2016;18:8
34. Schlett CL, Hendel T, Weckbach S, et al. Population-based imaging and radiomics: rationale and perspective of the German National Cohort MRI Study. Rofo 2016;188:652–661
35. Grundy SM. Pre-diabetes, metabolic syndrome, and cardiovascular risk. J Am Coll Cardiol 2012;59:635–643
36. Ford ES, Zhao G, Li C. Pre-diabetes and the risk for cardiovascular disease: a systematic review of the evidence. J Am Coll Cardiol 2010;55:1310–1317
37. Rijzewijk LJ, van der Meer RW, Lamb HJ, et al. Altered myocardial substrate metabolism and decreased diastolic function in nonischemic human diabetic cardiomyopathy: studies with cardiac positron emission tomography and magnetic resonance imaging. J Am Coll Cardiol 2009;54:1524–1532
38. van Heerebeek L, Hamdani N, Handoko ML, et al. Diastolic stiffness of the failing diabetic heart: importance of fibrosis, advanced glycation end products, and myocyte resting tension. Circulation 2008;117:43–51
39. Fox CS, Massaro JM, Hoffmann U, et al. Abdominal visceral and subcutaneous adipose tissue compartments: association with metabolic risk factors in the Framingham Heart Study. Circulation 2007;116:39–48
40. Rinella ME. Nonalcoholic fatty liver disease: a systematic review. JAMA 2015;313:2263–2273
41. Weckbach S, Findeisen HM, Schoenberg SO, et al. Systemic cardiovascular complications in patients with long-standing diabetes mellitus: comprehensive assessment with whole-body magnetic resonance imaging/magnetic resonance angiography. Invest Radiol 2009;44:242–250
42. Shah RV, Kwong R. Tissue characterization with cardiac MR imaging: a new hope for improving the cardiac outlook of patients with impaired fasting glucose? Radiology 2012;262:742–745
43. Trusheim MR, Berndt ER, Douglas FL. Stratified medicine: strategic and economic implications of combining drugs and clinical biomarkers. Nat Rev Drug Discov 2007;6:287–293
44. Yip SS, Aerts HJ. Applications and limitations of radiomics. Phys Med Biol 2016;61:R150–R166